frontiers | Frontiers in Environmental Science

TYPE Perspective
PUBLISHED 07 December 2022
DOI 10.3389/fenvs.2022.1084623

OPEN ACCESS

EDITED BY
Rajendra Prasad Singh,
Southeast University, China

REVIEWED BY
Sunny Sharma,
Dr. Yashwant Singh Parmar University of Horticulture and Forestry, India
Himanshu Gupta,
IFTM University, India
Chuanyu Gao,
Northeast Institute of Geography and Agroecology (CAS), China

*CORRESPONDENCE
Amit Kumar,
amitkdah@nuist.edu.cn
Zhi-Guo Yu,
zhiguo.yu@nuist.edu.cn

SPECIALTY SECTION
This article was submitted to Water and Wastewater Management, a section of the journal Frontiers in Environmental Science

RECEIVED 30 October 2022
ACCEPTED 21 November 2022
PUBLISHED 07 December 2022

CITATION
Liu Y-X, Abdela KA, Tang Z-N, Yu J-Y, Zhou X-D, Kumar A and Yu Z-G (2022), Impacts of surface water interchange between urban rivers and fish ponds in Chu river of Nanjing, China: A potential cause of greenhouse gas emissions. *Front. Environ. Sci.* 10:1084623. doi: 10.3389/fenvs.2022.1084623

Impacts of surface water interchange between urban rivers and fish ponds in Chu river of Nanjing, China: A potential cause of greenhouse gas emissions

Yi-Xuan Liu[1], Kemal Adem Abdela[1], Zhen-Ni Tang[1], Jie-Yu Yu[1], Xu-Dong Zhou[2], Amit Kumar[1]* and Zhi-Guo Yu[1]*

[1]Key Laboratory of Hydrometeorological Disaster Mechanism and Warning, Ministry of Water Resources/School of Hydrology and Water Resources, Nanjing University of Information Science and Technology, Nanjing, Jiangsu, China, [2]Nanjing Hydraulic Research Institute, Nanjing, China

Surface water interchange between aquaculture ponds and urban rivers is commonly used for the abatement of water pollution and regulating ecological services. Although, underlying impact of surface water interchange for greenhouse gas (GHG) emissions is yet to be explored. In this study, sediment microcosm incubation and field observation has been employed to understand the impact of surface water interchange on GHG potential over aquaculture ponds and urban rivers, and further characterize their underlying mechanism. Results showed that Fish pond$_{interchange}$ (P_{int}) and Chu River riparian (CRR) exhibit a similar variation pattern of GHG emission rate. Consequently, annual accumulative emissions of methane, carbon dioxide, and nitrous oxide of CRR were 0.89, 2.1, and 20.83 folds than that of P_{int}, respectively. For the incubation experiment, primarily it was assessed that fish-pond-overlying water treatments had larger accumulative GHG emissions than deionized water treatments, which is in agreement with the field observation. Secondly, the process of surface water interchange altered the concentrations of nutrients in benthic sediment from both sites of CRR and P_{int}, thereby increased the GHG accumulative in the CRR and showing reciprocate results in case of P_{int}. This study could be helpful to reduce the potential GHG emissions from urban freshwater bodies in the future by adopting strategic mitigation measures like catchment area treatment plans in the vicinity of urban river catchment.

KEYWORDS

surface water interchange, aquaculture ponds, urban rivers, greenhouse gases emissions, microcosm incubation

Introduction

In general, freshwater aquaculture ponds are utilized for agriculture farming where river water is used for life-supporting activities. But now a days they emit significant sources of greenhouse gas (GHG) emissions such as methane (CH_4), carbon dioxide (CO_2), and nitrous oxide (N_2O) (Yuan et al., 2019; Zhang et al., 2021). Rivers (particularly urban rivers) transport a substantial amount of nutrients, which may potentially lead to continually GHG emissions (Apelgren et al., 2019), In general, nutrient load of urban rivers has been altered considerably by domestic sewage, industrial effluents, storm-induced runoff (Garcia et al., 2013). It has been demonstrated that CH_4, CO_2, and N_2O fluxes at the water-gas interface are often substantially higher in urban rivers than in naturally flowing rivers (Rosamond et al., 2012; Kumar et al., 2022a). The immoderate usage of aqua feeds and the production of agricultural wastes enhance freshwater eutrophication and the deposition of organic carbon (OC) in fish ponds (Bohnes et al., 2019). In addition to that, benthic sediments of the pond are excellent for the anaerobic decomposition of organic matter (OM) due to the low water velocity, thus many previous studies demonstrated that freshwater aquaculture ponds emit higher GHGs than urban water bodies (Kosten et al., 2020). For example, Nanjing, a major city in China, is located in a sub-tropical monsoon climatic zone with a large number of urban rivers and a sizable freshwater aquaculture industry (Cheng and Hu, 2012). Freshwater aquaculture ponds are frequently observed near urban rivers in cities (Houbraken et al., 2017). Notably, low residence time leads to the re-suspension of sediment particles resulting in OM and nutrients diffusing into the water. Moreover, re-suspended sediment moves to the opposite side of the water with the water flow (Huettel and Rusch, 2000). Thus the process of surface water interchange impacts the overall exchangeable sediment particles (Förstner, 2004). Following the stabilization of the flow velocity, sediment particles that migrate to the other side of the water are redeposited (Qian et al., 2011). Literature reveals that microbial activities in the benthic sediment are the key source of GHG (in particular CH_4 and N_2O) emissions in freshwater ecosystems (Conrad, 2020). Generally, surface water interchange exists between freshwater aquaculture ponds and urban rivers or lakes, but few studies have clarified the impact of this process on accumulative GHG emissions (Xu et al., 2021). Literature reveals numerous climatic factors and hydrochemical parameters reported yet which play an important role in GHG production and emissions in freshwater ecosystems. Out of which the major primary parameters (e.g., inputs of nutrients, dissolved oxygen, pH, chlorophyll-a), secondary (e.g., water temperature, wind velocity) parameters, and anthropogenic activities in the vicinity of the urban river and/or pond catchments exacerbate the complexity of the mechanisms influencing GHG emissions (Kumar et al., 2019; 2022b; Li et al., 2021). Therefore, it is difficult to comprehend how a particular factor affects these ecosystems' processes and overall carbon dynamics (Tangen et al., 2016).

Literature reveals that very few reported studies have highlighted the relationship between surface water interchange and GHG emissions. Although, this relationship is important to understand the key processes behind it and implement strategic mitigation solutions. The present study aimed to 1) characterize GHG emissions patterns of freshwater aquaculture pond and urban Chu river under a long-term surface water interchange; 2) determine the impact and underlying mechanism of urban Chu rivers-fish ponds based surface water interchange on benthic sediment GHG emissions This study provides baseline information for the global statistics of carbon and nitrogen budget over aquaculture.

Materials and methods

In this study, four sampling sites, including Chu River riparian (R), Hongshan Gate (C), Fish $pond_{interchange}$ (F), and Zero-interchange fish pond (D) were located downstream of the Chu River were selected (Supplementary Figure S1; Supplementary Table S1). Moreover, R and F were selected for monthly (May 2020 to April 2021) observations of GHG emissions at the water-air interface. The studied sites fall under the humid subtropical climate of the northern hemisphere, with an annual average temperature of 15.4°C whereas the highest annual extreme temperature was recorded 43°C (13 July 1934) and the lowest is −14°C (6 January 1955). The average lowest temperature is 1.6°C in January with a mean of 30.6°C in July. The wettest months of the year are typically June and July, whereas 55% of the annual rainfall is concentrated between May and August. Detailed methodologies adopted for this study have been provided in the Supplementary Section S1.1.

Results

In situ observation of greenhouse gas emissions

The sampling sites chosen for field observation and microcosm incubation have been shown in Table 1. Notably, long-term surface water interchange management strategy has been implemented before sampling at Chu River riparian (CRR) and Fish $pond_{interchange}$ (P_{int}) sampling sites. During a year of field observation (May 2020 to April 2021), the CH_4 emissions rate for the sampling site of P_{int} was found relatively low in summer and autumn, then it begins to rise in late autumn and reach a higher value during the winter and spring period. Similarly for CRR, the CH_4 emissions rate was determined as a high value in spring and exhibited an increasing trend in late

TABLE 1 Sample sites selection for field observation and microcosm incubation.

In situ work	Sites	Lab work	Sediment	Treatments
Field observation	Chu River riparian	Microcosm incubation	Chu River riparian	Deionized water
				Fish-pond-overlying water
				Artificial water
			Hongshan gate	Deionized water
				Fish-pond-overlying water
				Artificial water
	Fish $pond_{interchange}$		Fish $pond_{interchange}$	Deionized water
				Fish-pond-overlying water
				Artificial water
			Zero-interchange fish pond	Deionized water
				Fish-pond-overlying water
				Artificial water

autumn and winter. Peak emissions rate of P_{int} was observed to be high (2.79 mmol $m^{-2}{\cdot}d^{-1}$) in October, while the peak emissions rate of CRR was observed to be low (0.91 mmol $m^{-2}{\cdot}d^{-1}$) in April (Figure 1A), except for the period of nutrient replenishment for P_{int} in October and during the freezing periods (November to December), the emissions rate of CH_4 from the sample site of CRR was higher than those of sample site for P_{int} among monitoring period.

The temporal variability of CO_2 was performed for CRR and the highest CO_2 emissions rate (85.32 mmol $m^{-2}{\cdot}d^{-1}$) was found in November and found to be 1.32 folds higher than that of measured value for P_{int}. Further, it was determined that the peak CO_2 emissions rate (40.82 mmol $m^{-2}{\cdot}d^{-1}$) for P_{int} in February but highest emissions period ranged from September to next January. Although, CO_2 emissions rate for P_{int} was reported to be lower than that of CRR. In addition, N_2O emissions rate for P_{int} did not fluctuate much but highest value was 2.21 10^{-2} mmol $m^{-2}{\cdot}d^{-1}$ in July and the lowest value was −2.30 10^{-2} mmol $m^{-2}{\cdot}d^{-1}$ in November. Similarly for CRR, the N_2O emissions rate was observed to be higher from June to September and peaked (0.13 mmol $m^{-2}{\cdot}d^{-1}$) in September. Overall, field observation revealed that the annual accumulative CH_4, CO_2 and N_2O emissions for P_{int} were 185.95, 3,424.63, and 0.72 mmol m^{-2} respectively whereas for CRR it was observed to be 167.60, 7,197.92, and 14.52 mmol m^{-2}, respectively (Figures 1B,C).

Greenhouse gas emissions o microcosm incubation

In microcosm incubation, four sediment samples were collected *in situ*. The triplicate samples of each treatment were established with different supernatant solutions that include deionized water, fish-pond-overlying water and artificial water. Fish-pond-overlying water was collected for P_{int}, while artificial water was prepared with a nitrogen/phosphorous (N/P) ratio of ~1 from fish-pond-overlying water (for more details see supporting information in Supplementary Tables S1,S2). The microcosm incubation was operated for 50 days. During this course, all treatments showed an increasing trend in accumulative emissions. After 50-day of incubation, the GHG production rates approached a steady state (Figure 2). Moreover, two sediment samples collected from aquaculture ponds (P_{int} and Zero-interchange fish pond) had considerably greater accumulative emissions for both CO_2 and CH_4, which was higher than that of sediment obtained from urban rivers (CRR and Hongshan gate). Comparatively, incubation of deionized water treatments for Hongshan gate sediment had higher CO_2 emissions than P_{int}. For aquaculture pond sediments, the accumulative GHG emissions for P_{int} sediment had much lower than those of Zero-interchange fish pond sediment. Notably, CRR sediment had higher accumulative emissions ofCH_4 and N_2O than that of incubated sediment of Hongshan gate. Besides, incubated sediment for CRR was observed to be more N_2O than that of P_{int} sediment, shown in Supplementary Table S3.

From the three different applied supernatant solutions for sediments incubations, all treatments with artificial water emitted more CH_4 than the others. Except for Hongshan gate, the highest accumulative CO_2 emissions were observed from fish-pond-overlying water treatments. For the accumulative N_2O emissions, no statistical significance was found among river sediments. While artificial water treatment emits more N_2O than other treatments for aquaculture ponds sediments (Figure 2; Supplementary Table S3).

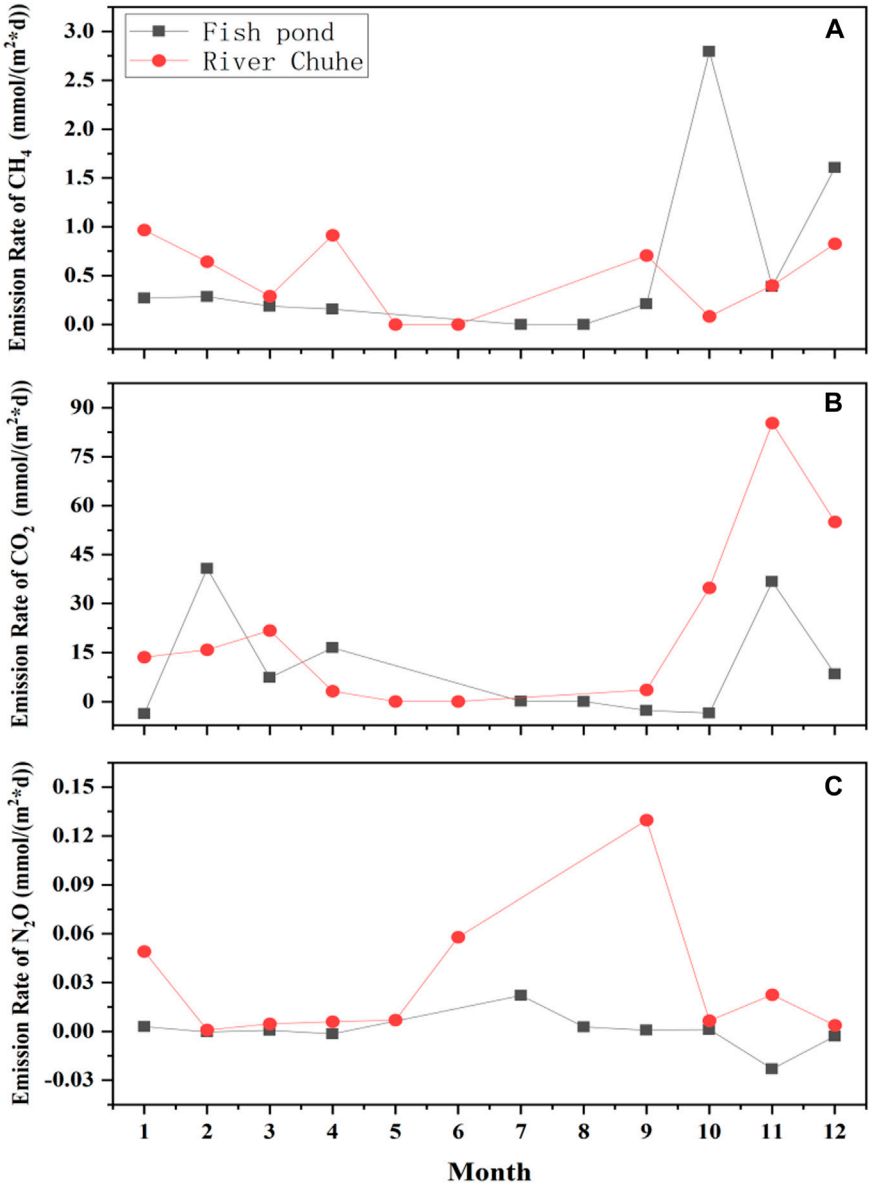

FIGURE 1
Temporal variability in GHG emissions rate during field observation, where **(A–C)** denotes the emissions rate of CH_4, CO_2, and N_2O respectively.

Methanogenic pathways for microcosm incubation experiments

Stable carbon isotope analysis was performed for the collected gases in the samples on 29th day of incubation. The abundance ratios and isotopic fractionation factor (αc) were calculated from the thousandth deviation of the actual sample from the standard sample. The isotopic fractionation factor of all samples was >1.055, (Supplementary Table S4), which indicates the occurrence of hydrogenotrophic methanogenesis (SI.Eq.S4).

Changes in hydrochemical factors during microcosm incubation

During the microcosm incubation, the highest concentrations of ammonium nitrogen (NH_4^+-N), nitrate nitrogen (NO_3^-N), dissolved organic matter (DOC) and dissolved inorganic matter (DIC) were found in Zero-interchange fish pond sediment treatment. The DOC and DIC concentration in all treatments of P_{int} sediment were higher than those of CRR sediments. For aquaculture ponds, concentrations

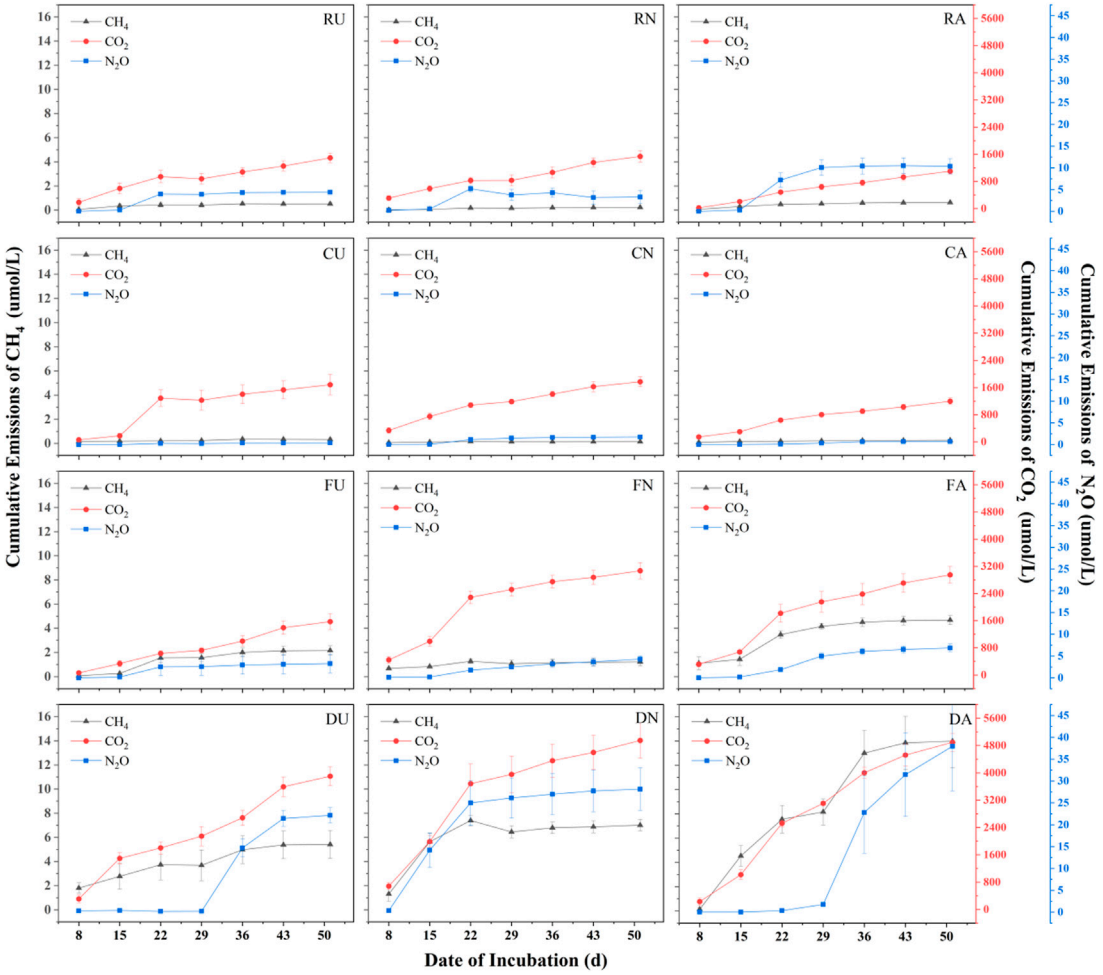

FIGURE 2
Changes in cumulative CH_4, CO_2 and N_2O emissions over 50 days for different treatments, where R, C, F, & D represent Chu River riparian sediment, Hongshan Gate sediment, Fish $pond_{interchange}$ sediment, D Zero-interchange fish pond sediment respectively. Moreover, U, N, and A represent deionized water treatment, fish-pond-overlying water treatment and artificial water treatment.

of NH_4^+-N and NO_3^--N were lower than those of CRR sediment in deionized water treatment and fish-pond-overlying water treatment. Noticeably, the total phosphorus (TP) concentration in all treatments of river sediments was higher than those of aquaculture ponds sediments, and the peak value was found in the treatments of Hongshan gate sediment (Table 2).

Spearman's correlation analysis was applied to the GHGs emissions rates and the concentrations of hydrochemical parameters, part of the correlations passed the significance test, but other correlations indicate the relations between factors as well (Figure 3). The results showed that the GHGs emissions rates were strongly negatively correlated with TP and C/N ratio, and weakly correlated with NH_4^+-N, while all other parameters showed a positive trend of correlation. A strong positive correlation (R^2: 0.7, $p < 0.05$) was obtained between CH_4 emissions rates and N/P ratio while a positive correlation between CO_2 emissions rates and DOC, CO_2 emissions rates and N/P ratio at degree of 0.64 and 0.67 ($p < 0.05$), respectively. In addition, N_2O emissions rates had a positive correlation with NO_3^--N (R^2: 0.56, $p < 0.05$) and a negative correlation for TP (R^2: 0.45, $p < 0.05$).

Chemical properties of organic matter

Fluorescence-parallel factor analysis of water samples was performed using the DOMFluor toolbox. The result showed that a total of five organic components in all samples, where C_1 represents approximately equal humic acid and fulvic acid, C_2 represents fulvic acid, C_3 represents fulvic acid and a trace of humic acid, C_4 represents tyrosine and certain protein-like

TABLE 2 Variation of hydrochemical parameter for different treatments in microcosm incubation.

Treatments	Sediment	DOC ($mmol·L^{-1}$)	DIC ($mmol·L^{-1}$)	TP ($mmol·L^{-1}$)	NH_4^+-N ($mmol·L^{-1}$)	NO_3^--N ($mmol·L^{-1}$)
Deionized water	Chu River Riparian	0.49	2.60	2.29 10^{-3}	6.39 10^{-3}	11.76 10^{-3}
	Hongshan Gate	0.47	2.87	2.13 10^{-3}	4.17 10^{-3}	6.95 10^{-3}
	Fish $pond_{interchange}$	0.59	2.83	1.94 10^{-3}	5.28 10^{-3}	13.32 10^{-3}
	Zero-interchange fish pond	0.78	3.28	2.71 10^{-3}	14.44 10^{-3}	17.32 10^{-3}
Fish pond overlying water	Chu River Riparian	0.68	3.06	2.49 10^{-3}	5.28 10^{-3}	17.58 10^{-3}
	Hongshan Gate	0.71	3.03	2.71 10^{-3}	3.33 10^{-3}	7.45 10^{-3}
	Fish $pond_{interchange}$	0.79	3.14	2.10 10^{-3}	4.72 10^{-3}	16.13 10^{-3}
	Zero-interchange fish pond	1.04	3.61	2.03 10^{-3}	12.50 10^{-3}	33.69 10^{-3}
Artificial water	Chu River Riparian	0.47	2.58	2.42² 10^{-3}	10.00 10^{-3}	12.97 10^{-3}
	Hongshan Gate	0.47	2.78	2.26 10^{-3}	3.89 10^{-3}	9.13 10^{-3}
	Fish $pond_{interchange}$	0.57	2.85	2.03 10^{-3}	6.11 10^{-3}	17.71 10^{-3}
	Zero-interchange fish pond	0.87	3.68	2.42 10^{-3}	25.00 10^{-3}	25.11 10^{-3}

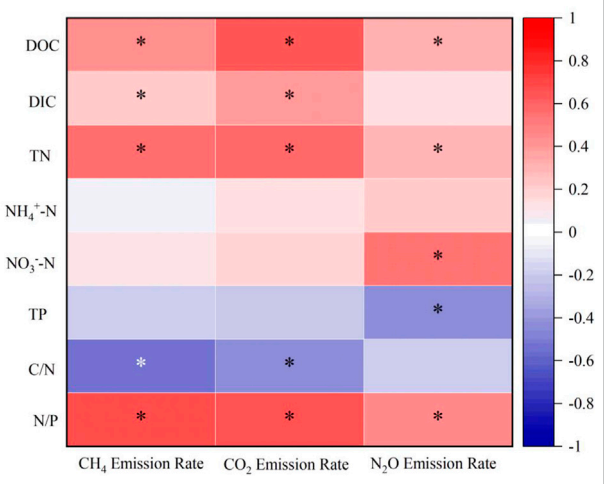

FIGURE 3
Correlation between GHG emission rates and hydrochemical parameters for microcosm incubation, where * represent the p values (<0.05) of significant analysis.

fractions, and C_5 represent aromatic protein and microbiological by-products (Figure 4). Notably, C_1, C_2, and C_3 were the components that existed in all sediment samples, while C_4 was found only in samples of Hongshan Gate sediment, and C_5 was found only in samples of the Zero-interchange fish pond, which means a similar distribution of components occurred in samples of CRR and P_{int} sediments. Figure 5 indicated that the relative content of C_1 increased before the 22nd day of incubation, from a mean value of all treatment groups of 31.25% to a mean value of 49.25%. However, decreased from the 15th day of incubation, the mean value at the end was 41.25%, whereas the variation trend of relative content of C_3 was diametrically opposite to that of C_1, decreasing from a mean value of 38.78% to a mean value of 19.5%, then starting increasing, the mean value at the end was of 26%, the relative content of C_2 was lower than the other two common fractions, varies from 28% to 36%.

In all treatments, the content of OM from the sediment was lower at the end of incubation than its initial value (Supplementary Table S5), proving that the incubation procedure significantly depleted the OM. In terms of sediments, the consumption rate of OM in descending order was Zero-interchange fish pond sediment, P_{int} sediment, CRR sediment and Hongshan Gate sediment. In terms of supernatants, the consumption rate of OM was found in descending order with deionized water treatment, fish-pond-overlying water treatment, and artificial water treatment.

Discussion

Emissions pattern of CH_4, CO_2, and N_2O

During the field campaign, the period of high emissions was commonly found in the summer and autumn seasons. Moreover, CRR and P_{int} showed high CH_4 and CO_2 emissions periods between October to April (Yang et al., 2018b; Sieczko et al., 2020). It could be attributed to fishery management that bait, fresh fry, and fish bait were dosed into P_{int} in late summer while other aquaculture ponds popularly dosed for the same in the spring

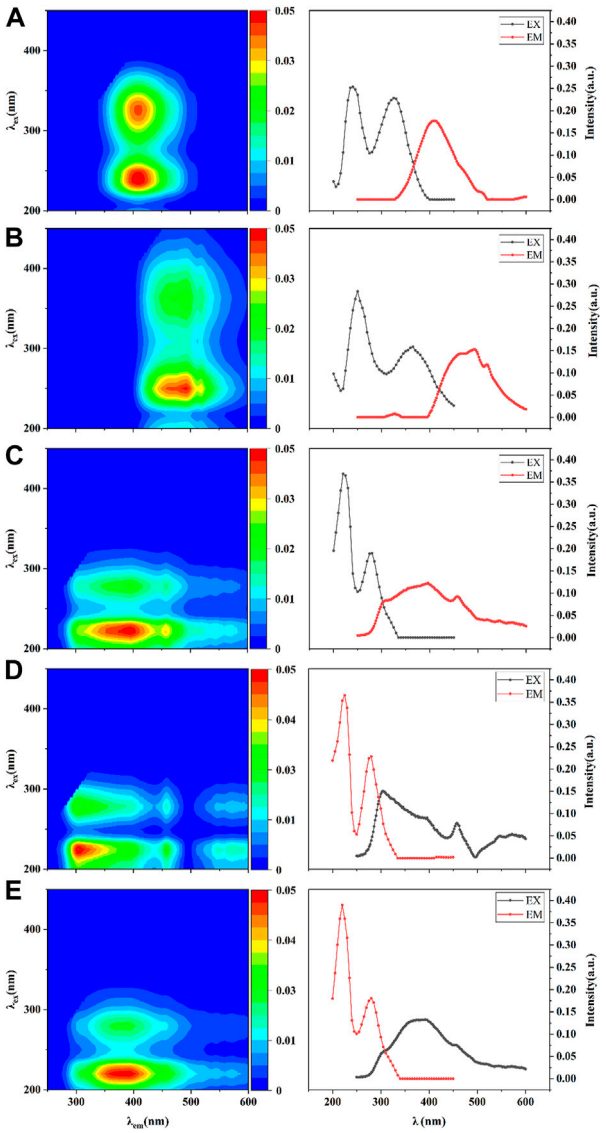

FIGURE 4
Fluorescence organic components of Fluorescence-PARAFAC; **(A–E)** denotes the five organic components (C_1-C_5) and the variation with the emissions wavelength (EM) and excitation wavelength (EX).

(Yang et al., 2017; 2018a). For P_{int} site, the input of nutrients in autumn and early winter ensured the metabolism and growth of organisms in pond even during the freezing season. Generally, it provides a substrate for the aerobic respiration of OM in the sediment which results in higher emissions of CH_4 and CO_2 in autumn and winter (Hill et al., 2017). The high loading of nutrients in P_{int} sediment might potentially be released into the water due to the long-term process of surface water interchange that accumulated into CRR. In addition, the observed increase in GHG emissions rates favors due to water pollution of CRR (Yu et al., 2013; Wang et al., 2015). Thus, surface water interchange management exhibits a similar emission pattern for CRR and $P_{int.}$ The elevated N_2O emissions from June to October of CRR coincide with the results of previous studies on river riparians (Cole and Caraco, 2001). It could be due to input of nitrogen from household and industrial waste from upstream catchment of Chu River thereby increasing the N_2O emission rate. Further supportive made by rising groundwater levels over Chu riparian (Bange et al., 2019).

Field observation reveals that microcosm incubation experiments could be employed for further understanding the underlying mechanism of GHG emission patterns. In aspect of sediment chemical properties, in contrast to Hongshan gate sediment, the transportation of OM and nutrients through runoffs between P_{int} and CRR contribute high CO_2 and CH_4 emissions. Contrastingly, for Zero-interchange fish pond sediment, the process of surface water interchange reduces the accumulative GHG emissions of P_{int} sediment. In addition, CRR sediment had apparent accumulative N_2O emissions which could be attributed to the large input of surface runoffs (Fagervold et al., 2014; Bange et al., 2019).

From the perspective of applied overlying water, fish-pond-overlying water enriched with OM had the highest accumulative CO_2 emissions. However, the deposition of OM increases the carbon buried in benthic sediment and is further utilized in decomposition process (Hu et al., 2022). The presence of electron acceptors in fish-pond-overlying water, such as NO_3^- affects methanogenesis and thus CH_4 was found to be relatively low (Raghoebarsing et al., 2006). Besides, no clear CH_4 inhibition was found in artificial water treatment which might be due to excessive NH_4^+-N. Generally, nitrogen and phosphorus inputs promoted the decomposition of OM, resulting in high GHG emissions from artificial water treatments (Tao et al., 2018). However, the substantial storage of carbon in both sediment and supernatant had made a positive impact to reduce CH_4 emissions, thus fish-pond-overlying water treatments of Zero-interchange fish pond sediment had the highest CH_4 emissions. The transformation between NH_4^+-N and NO_3^- -N over the water-sediment interface is the key reason for N_2O emissions (Wang et al., 2007; Howard, 2015). The addition of NH_4^+-N in artificial water increases the nitrification rate in the corresponding treatment which leads to higher N_2O flux within artificial water treatments. Subsequently, fish-pond-overlying water treatments exhibit high accumulative GHG emissions than that deionized water treatments which supports the viewpoint as a consequence of surface water interchange.

Acetotrophic methanogenesis and hydrogenotrophic methanogenesis are well-recognized for CH_4 production pathways under waterlogged conditions (Conrad et al., 2010; Mach et al., 2015). The present results are in agreement with CH_4 production mainly *via* hydrogenotrophic methanogens pathways which coincide with reported founding in incubated lake

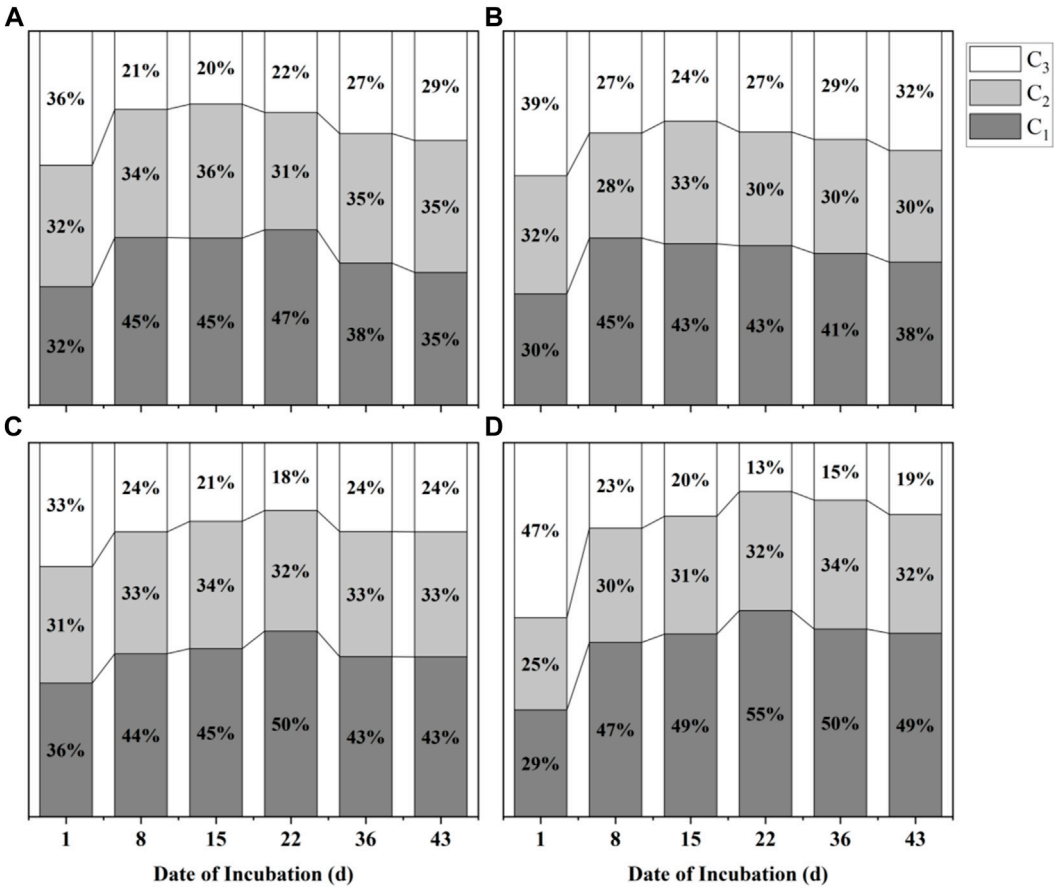

FIGURE 5
Temporal variation of organic components (%; C_1, C_2 and C_3) from four sediments are plotted against time, where **(A–D)** represent the Chu River riparian sediment, Hongshan Gate sediment, Fish $pond_{interchange}$ sediment and Zero-interchange fish pond sediment.

sediments (Avery et al., 2003). It is interpreted in the previous studies that the different energy sources may govern various methanogenic pathways (Glissmann et al., 2004. However, the present study ascertains no significant influence over the methanogenic pathway due to variation in overlaying water treatments.

Interactive effect of surface water interchanges with greenhouse gas emission and water chemistry

As a consequence of a long-term surface water interchange, nutrient loading in the benthic sediment of CRR has increased accordingly, while that of sediment of P_{int} had been diluted which complies with the variation of GHG emission. The input of substantial industrial wastewater is responsible for the concentrations of NH_4^+-N and NO_3^--N in treatments of CRR sediment and was found to be higher than those of P_{int} sediment (Rosamond et al., 2012; Zhang et al., 2021). The changes in the hydrochemical indicators altered the distribution of chemicals in the benthic sediment, which would have a potential impact on GHG emissions.

Apparently in this study, the variation of water chemistry has a strong impact on GHG emissions. Previous studies interpreted that transforming nitrogen would provide more substrate for microbial decomposition resulting significant amount of CH_4 and CO_2 emissions (Stiles et al., 2018). Besides, it has been reported that the presence of phosphate could either promote GHG production or inhibits methanogenesis, which is determined by total amount of loaded phosphor (Zhang et al., 2011). Current results had a positive correlation between GHG emission and TN loading, while TP was negatively correlated (Raghoebarsing et al., 2006). The higher concentration of TP in samples of Hongshan Gate sediment might inhibit the decomposition of OM, which inhibits the emissions of all

three GHG (Zhang et al., 2011). Furthermore, it has been demonstrated that lower C/N ratios lead to the consumption of high amounts of organic nitrogen which promotes microbial activity leading to high GHG emissions (Zhang W et al., 2022).

Relation between chemical properties of dissolved organic matter and greenhouse gas emissions

Dissolved organic matter (DOM) is ubiquitous and it affects fundamental biogeochemical processes in freshwater ecosystems. In general, PARAFAC method was employed to interpret the key mechanism of the DOM and underlying GHG emission (Ding et al., 2022). Humic acid increases the ability of benthic sediment carbon burial and inhibits GHG emissions, while fulvic acid enhances the effectiveness of biological processes thus promoting the decomposition of OM. During the analysis, it was found that component C_1 had the highest proportion of fulvic acid, compared with other two common components (Yu et al., 2014). Since the proportion of component C_1 among the three common components was the highest in Zero-interchange fish pond sediment explicates the highest accumulative GHG emissions in the sediment. Component C_5 represents microbial by-products in Zero-interchange fish pond sediment which indicates the decomposition of OM resulting in high GHG emissions (Kimbrough and Dickhut, 2006). Theoretically, OM in urban river sediments ought to be homologous, and thus the process of surface water exchange might lead to the result that C_4 component was only derived in the sediment of Hongshan gate. These processes altered the composition of OM for CRR thus altering the potential of GHG emissions.

Fluorescence index (FI) and Humization index (HIX) are used frequently to evaluate DOM quality. Thus, FI and HIX were also used for DOM over incubation treatment, the results were given in Supplementary Table S6. Obtained FI value was higher than 1.5 in all treatments which indicates that the carbon within the studied incubation was mainly microbially active carbon, instead of carbon derived from terrestrial sources (Broder et al., 2017). In addition, obtained Humization index (HIX) value close to 1 for all treatments, indicates that DOM contains more humified compounds which potentially highlight an active carbon pool that contributes to GHG emission (D'Andrilli et al., 2022). It is suggested that the characterization of DOM is fundamental to understand carbon cycling and dynamics in aquatic ecosystems. Moreover, fluorescence-PARAFAC analysis provided the scientific basis for interpreting variation in GHG emissions therefore further studies need to be explored to fill the knowledge gap of organic carbon turnover at the terrestrial-aquatic interface.

Conclusion

This study indicates the process of surface water interchange between aquaculture ponds and urban rivers which increased the potential of GHG emissions in the benthic sediments. Consequently reduced the GHG emission rates of aquaculture pond sediments. Result reveal that annual accumulative emissions of CH_4, CO_2, and N_2O for Chu River riparian were 0.89, 2.1, and 20.83 folds than that of P_{int}, respectively. However, the potential artifacts and consequences are not considered in this study. Besides, the microcosm incubation exhibits a strong agreement with field observation. Moreover, during surface water interchange, input and output of organic matter (OM) play a crucial role to understand the potential changing of GHG emissions in urban rivers and aquaculture ponds sediments. Fluorescence-PARAFAC findings indicates that long-term surface water interchange processes not only change the concentration of OM in the sediment but also change the composition of the organic component. Consequently, it may lead to significant variations in GHG emissions. This study suggested that the surface water management regime may lead to high GHG emissions from urban freshwater which might underestimate the carbon emission budget over the freshwater ecosystem.

Data availability statement

The original contributions presented in the study are included in the article/Supplementary Material, further inquiries can be directed to the corresponding authors.

Author contributions

Conceptualization: Y-XL Formal analysis and first draft: Y-XL, KA, Z-NT, and J-YY Review and editing: X-DZ, AK, and Z-GY Project funding: Z-GY.

Funding

This paper was supported by the National Natural Science Foundation of China (Grant number: 41877337, 41601090).

Acknowledgments

The authors are thankful to the members of the Key Laboratory of Hydrometeorological Disaster Mechanism and Warning to help to finish our experiments.

Conflict of interest

The authors declare that the research was conducted in the absence of any commercial or financial relationships that could be construed as a potential conflict of interest.

Publisher's note

All claims expressed in this article are solely those of the authors and do not necessarily represent those of their affiliated organizations, or those of the publisher, the editors and the reviewers. Any product that may be evaluated in this article, or claim that may be made by its manufacturer, is not guaranteed or endorsed by the publisher.

Supplementary material

The Supplementary Material for this article can be found online at: https://www.frontiersin.org/articles/10.3389/fenvs.2022.1084623/full#supplementary-material

References

Apelgren, P., Amoroso, M., Säljö, K., Montelius, M., Lindahl, A., Stridh Orrhult, L., et al. (2019). Dissolved organic carbon and nitrogen release from boreal Holocene permafrost and seasonally frozen soils of Alaska. *Mat. Today Proc.* 27, 0–31. doi:10.1088/1748-9326/aac4ad

Avery, G. B., Shannon, R. D., White, J. R., Martens, C. S., and Alperin, M. J. (2003). Controls on methane production in a tidal freshwater estuary and a peatland: Methane production via acetate fermentation and CO_2 reduction. *Biogeochemistry* 62, 19–37. doi:10.1023/A:1021128400602

Bange, H. W., Sim, C. H., Bastian, D., Kallert, J., Kock, A., Mujahid, A., et al. (2019). Nitrous oxide (N_2O) and methane (CH_4) in rivers and estuaries of northwestern Borneo. *Biogeosciences* 16, 4321–4335. doi:10.5194/bg-16-4321-2019

Bohnes, F. A., Hauschild, M. Z., Schlundt, J., and Laurent, A. (2019). Life cycle assessments of aquaculture systems: A critical review of reported findings with recommendations for policy and system development. *Rev. Aquac.* 11, 1061–1079. doi:10.1111/raq.12280

Broder, T., Knorr, K. H., and Biester, H. (2017). Changes in dissolved organic matter quality in a peatland and forest headwater stream as a function of seasonality and hydrologic conditions. *Hydrol. Earth Syst. Sci.* 21, 2035–2051. doi:10.5194/hess-21-2035-2017

Cheng, H., and Hu, Y. (2012). Improving China's water resources management for better adaptation to climate change. *Clim. Change* 112, 253–282. doi:10.1007/s10584-011-0042-8

Cole, J. J., and Caraco, N. F. (2001). Emissions of nitrous oxide (N_2O) from a tidal, freshwater river, the Hudson River, New York. *Environ. Sci. Technol.* 35, 991–996. doi:10.1021/es0015848

Conrad, R., Klose, M., Claus, P., and Enrich-Prast, A. (2010). Methanogenic pathway, ^{13}C isotope fractionation, and archaeal community composition in the sediment of two clear-water lakes of Amazonia. *Limnol. Oceanogr.* 55, 689–702. doi:10.4319/lo.2009.55.2.0689

Conrad, R. (2020). Methane production in soil environments—anaerobic biogeochemistry and microbial life between flooding and desiccation. *Microorganisms* 8, 881. doi:10.3390/microorganisms8060881

D'Andrilli, J., Silverman, V., Buckley, S., and Rosario-Ortiz, F. L. (2022). Inferring ecosystem function from dissolved organic matter optical properties: A critical review. *Environ. Sci. Technol.* 56, 11146–11161. doi:10.1021/acs.est.2c04240

Ding, H., Hu, Q., Cai, M., Cao, C., and Jiang, Y. (2022). Effect of dissolved organic matter (DOM) on greenhouse gas emissions in rice varieties. *Agric. Ecosyst. Environ.* 330, 107870–107926. doi:10.1016/j.agee.2022.107870

Fagervold, S. K., Bourgeois, S., Pruski, A. M., Charles, F., Kerhervé, P., Vétion, G., et al. (2014). River organic matter shapes microbial communities in the sediment of the Rhône prodelta. *ISME J.* 8, 2327–2338. doi:10.1038/ismej.2014.86

Förstner, U. (2004). Sediment dynamics and pollutant mobility in rivers: An interdisciplinary approach. *Lakes &amp. Reserv.* 9, 25–40. doi:10.1111/j.1440-1770.2004.00231.x

Garcia, S. N., Clubbs, R. L., Stanley, J. K., Scheffe, B., Yelderman, J. C., and Brooks, B. W. (2013). Comparative analysis of effluent water quality from a municipal treatment plant and two on-site wastewater treatment systems. *Chemosphere* 92, 38–44. doi:10.1016/j.chemosphere.2013.03.007

Glissmann, K., Chin, K. J., Casper, P., and Conrad, R. (2004). Methanogenic pathway and archaeal community structure in the sediment of eutrophic Lake Dagow: Effect of temperature. *Microb. Ecol.* 48, 389–399. doi:10.1007/s00248-003-2027-2

Hill, B. H., Elonen, C. M., Herlihy, A. T., Jicha, T. M., and Mitchell, R. M. (2017). A synoptic survey of microbial respiration, organic matter decomposition, and carbon efflux in U.S. streams and rivers. *Limnol. Oceanogr.* 62, S147–S159. doi:10.1002/lno.10583

Houbraken, M., Habimana, V., Senaeve, D., López-Dávila, E., and Spanoghe, P. (2017). Multi-residue determination and ecological risk assessment of pesticides in the lakes of Rwanda. *Sci. Total Environ.* 576, 888–894. doi:10.1016/j.scitotenv.2016.10.127

Howard, T. (2015). Comment on "methane emissions from process equipment at natural gas production sites in the United States: Pneumatic controllers. *Environ. Sci. Technol.* 49, 3981–3982. doi:10.1021/acs.est.5b00507

Hu, A., Choi, M., Tanentzap, A. J., Liu, J., Jang, K. S., Lennon, J. T., et al. (2022). Ecological networks of dissolved organic matter and microorganisms under global change. *Nat. Commun.* 13, 3600–3615. doi:10.1038/s41467-022-31251-1

Huettel, M., and Rusch, A. (2000). Transport and degradation of phytoplankton in permeable sediment. *Limnol. Oceanogr.* 45, 534–549. doi:10.4319/lo.2000.45.3.0534

Kimbrough, K. L., and Dickhut, R. M. (2006). Assessment of polycyclic aromatic hydrocarbon input to urban wetlands in relation to adjacent land use. *Mar. Pollut. Bull.* 52, 1355–1363. doi:10.1016/j.marpolbul.2006.03.022

Kosten, S., Almeida, R. M., Barbosa, I., Mendonça, R., Santos Muzitano, I., Sobreira Oliveira-Junior, E., et al. (2020). Better assessments of greenhouse gas emissions from global fish ponds needed to adequately evaluate aquaculture footprint. *Sci. Total Environ.* 748, 141247. doi:10.1016/j.scitotenv.2020.141247

Kumar, A., Mishra, S., Bakshi, S., Upadhyay, P., and Thakur, T. K. (2022a). Response of eutrophication and water quality drivers on greenhouse gas emissions in lakes of China: A critical analysis. *Ecohydrology*, e2483. doi:10.1002/eco.2483

Kumar, A., Upadhyay, P., and Prajapati, S. K. (2022b). Impact of Microplastics on riverine greenhouse gas emissions- A View point. *Env. Sci. Pollut. Res.* 29 (54). doi:10.1007/s11356-022-23929-2

Kumar, A., Yang, T., and Sharma, M. P. (2019). Greenhouse gas measurement from Chinese freshwater bodies: A review. *J. Clean. Prod.* 233, 368–378. doi:10.1016/j.jclepro.2019.06.052

Li, Y., Shang, J., Zhang, C., Zhang, W., Niu, L., Wang, L., et al. (2021). The role of freshwater eutrophication in greenhouse gas emissions: A review. *Sci. Total Environ.* 768, 144582. doi:10.1016/j.scitotenv.2020.144582

Mach, V., Blaser, M. B., Claus, P., Chaudhary, P. P., and Rulík, M. (2015). Methane production potentials, pathways, and communities of methanogens in vertical sediment profiles of river Sitka. *Front. Microbiol.* 6, 506–512. doi:10.3389/fmicb.2015.00506

Qian, J., Zheng, S. S., Wang, P. F., and Wang, C. (2011). Experimental study on sediment resuspension in taihu lake under different hydrodynamic disturbances. *J. Hydrodyn.* 23, 826–833. doi:10.1016/S1001-6058(10)60182-5

Raghoebarsing, A. A., Pol, A., Van De Pas-Schoonen, K. T., Smolders, A. J. P., Ettwig, K. F., Rijpstra, W. I. C., et al. (2006). A microbial consortium couples anaerobic methane oxidation to denitrification. *Nature* 440, 918–921. doi:10.1038/nature04617

Rosamond, M. S., Thuss, S. J., and Schiff, S. L. (2012). Dependence of riverine nitrous oxide emissions on dissolved oxygen levels. *Nat. Geosci.* 5, 715–718. doi:10.1038/ngeo1556

Sieczko, A. K., Thanh Duc, N., Schenk, J., Pajala, G., Rudberg, D., Sawakuchi, H. O., et al. (2020). Diel variability of methane emissions from lakes. *Proc. Natl. Acad. Sci. U. S. A.* 117, 21488–21494. doi:10.1073/pnas.2006024117

Stiles, W. A. V., Rowe, E. C., and Dennis, P. (2018). Nitrogen and phosphorus enrichment effects on CO_2 and methane fluxes from an upland ecosystem. *Sci. Total Environ.* 618, 1199–1209. doi:10.1016/j.scitotenv.2017.09.202

Tangen, B. A., Finocchiaro, R. G., Gleason, R. A., and Dahl, C. F. (2016). Greenhouse gas fluxes of a shallow lake in south-central north Dakota, USA. *Wetlands* 36, 779–787. doi:10.1007/s13157-016-0782-3

Tao, B., Liu, C., Zhang, B., and Dong, J. (2018). Effects of inorganic and organic nitrogen additions on CO_2 emissions in the coastal wetlands of the Yellow River Delta, China. *Atmos. Environ. X.* 185, 159–167. doi:10.1016/j.atmosenv.2018.05.009

Wang, D., Chen, Z., Wang, J., Xu, S., Yang, H., Chen, H., et al. (2007). Summer-time denitrification and nitrous oxide exchange in the intertidal zone of the Yangtze Estuary. *Estuar. Coast. Shelf Sci.* 73, 43–53. doi:10.1016/j.ecss.2006.11.002

Wang, J., Chen, N., Yan, W., Wang, B., and Yang, L. (2015). Effect of dissolved oxygen and nitrogen on emission of N_2O from rivers in China. *Atmos. Environ. X.* 103, 347–356. doi:10.1016/j.atmosenv.2014.12.054

Xu, Y., Chan, F. K. S., Johnson, M., Stanton, T., He, J., Jia, T., et al. (2021). Microplastic pollution in Chinese urban rivers: The influence of urban factors. *Resour. Conserv. Recycl.* 173, 105686. doi:10.1016/j.resconrec.2021.105686

Yang, P., Lai, D. Y. F., Huang, J. F., and Tong, C. (2018a). Effect of drainage on CO_2, CH_4, and N_2O fluxes from aquaculture ponds during winter in a subtropical estuary of China. *J. Environ. Sci.* 65, 72–82. doi:10.1016/j.jes.2017.03.024

Yang, P., Lai, D. Y. F., Jin, B., Bastviken, D., Tan, L., and Tong, C. (2017). Dynamics of dissolved nutrients in the aquaculture shrimp ponds of the Min River estuary, China: Concentrations, fluxes and environmental loads. *Sci. Total Environ.* 603–604, 256–267. doi:10.1016/j.scitotenv.2017.06.074

Yang, P., Zhang, Y., Lai, D. Y. F., Tan, L., Jin, B., and Tong, C. (2018b). Fluxes of carbon dioxide and methane across the water–atmosphere interface of aquaculture shrimp ponds in two subtropical estuaries: The effect of temperature, substrate, salinity and nitrate. *Sci. Total Environ.* 635, 1025–1035. doi:10.1016/j.scitotenv.2018.04.102

Yu, H., Song, Y., Liu, R., Xi, B., Du, E., and Xiao, S. (2014). Variation of dissolved fulvic acid from wetland measured by UV spectrum deconvolution and fluorescence excitation-emission matrix spectrum with self-organizing map. *J. Soils Sediments* 14, 1088–1097. doi:10.1007/s11368-014-0869-5

Yu, Z., Deng, H., Wang, D., Ye, M., Tan, Y., Li, Y., et al. (2013). Nitrous oxide emissions in the Shanghai river network: Implications for the effects of urban sewage and IPCC methodology. *Glob. Chang. Biol.* 19, 2999–3010. doi:10.1111/gcb.12290

Yuan, J., Xiang, J., Liu, D., Kang, H., He, T., Kim, S., et al. (2019). Rapid growth in greenhouse gas emissions from the adoption of industrial-scale aquaculture. *Nat. Clim. Chang.* 9, 318–322. doi:10.1038/s41558-019-0425-9

Zhang, T., Zhu, W., Mo, J., Liu, L., and Dong, S. (2011). Increased phosphorus availability mitigates the inhibition of nitrogen deposition on CH_4 uptake in an old-growth tropical forest, southern China. *Biogeosciences* 8, 2805–2813. doi:10.5194/bg-8-2805-2011

Zhang, W., Kang, X., Kang, E., Audet, J., Davidson, T. A., Zhang, X., et al. (2022). Soil water content, carbon, and nitrogen determine the abundances of methanogens, methanotrophs, and methane emission in the Zoige alpine wetland. *J. Soils Sediments* 22, 470–481. doi:10.1007/s11368-021-03043-5

Zhang, W., Li, H., Xiao, Q., and Li, X. (2021). Urban rivers are hotspots of riverine greenhouse gas (N_2O, CH_4, CO_2) emissions in the mixed-landscape chaohu lake basin. *Water Res.* 189, 116624. doi:10.1016/j.watres.2020.116624